NOTES AND CORRESPONDENCE

Further FGGE Forecasts for Amazon Basin Rainfall

JULIO BUCHMANN

Dept. de Meteorologia-Instituto do Geociencias, Universidade Federal do Rio de Janeiro, Rio de Janeiro, Brazil

JAN PAEGLE AND LAWRENCE BUJA

Dept. of Meteorology, University of Utah, Salt Lake City, Utah

R. E. DICKINSON

National Center for Atmospheric Research, Boulder, Colorado

3 August 1988 and 30 November 1988

ABSTRACT

A series of experiments using real-data general circulation model integrations is performed to study the impact of remote tropical Pacific heating modifications upon the rainfall over the Amazon Basin. In one set of experiments, a heating term is added to the thermodynamic equation in the western tropical Pacific Ocean, and in the second set, the sea surface temperatures are cooled in the eastern Pacific Ocean. The rainfall of northern sections of South America decreases in the first set of experiments and increases in the second set of experiments. Examination of the circulation changes for the second set of experiments suggests that the remote links occur through equatorially trapped flow modifications, perhaps related to the east–west Walker cells, rather than through midlatitude teleconnections via Hadley cells. The time evolution of these patterns suggests them to be clearly relevant for medium range weather prediction in the tropics.

1. Background

The relationship between long term anomalies of rainfall over tropical South America and the El Niño–Southern Oscillation (ENSO) has attracted considerable interest in recent years (Hastenrath and Heller 1977; Kousky et al. 1984; Rogers 1987; Ropelewski and Halpert 1987; Aceituno 1988; Aragoa 1986). However, there have been few real-data forecast experiments focusing upon predictability of ENSO influences on rainfall over South America. Buchmann et al. (1986) presented 20 real data integrations of a global general circulation model which demonstrated that the influence of enhanced eastern Pacific heating changes upon the rainfall of the Amazon Basin is predictable in a series of 10-day integrations. The results are in approximate agreement with observational studies which suggest that remote influences over the Pacific Ocean and the North Atlantic may produce modifications in the rainfall of northeastern Brazil, and perhaps contribute to the severe droughts occasionally observed there (Walker 1928; Namias 1972; Kousky et al. 1984; Rogers 1987).

This study presents further general circulation model experiments designed to investigate the influence of atmospheric changes over the Pacific Ocean upon the precipitation of the Amazon Basin. Buchmann et al. (1986; hereafter referred to as I) only performed experiments in which the tropical heating was increased over the eastern Pacific Ocean. They did not study whether the rainfall of tropical South America would be changed by Pacific heating enhancements that are imposed farther to the west, nor did they investigate the consequences of below average east Pacific temperature (as typically occurs in anti-El Niño years). The latter question was partly answered in a series of Northern Spring experiments performed by Paegle et al. (1987), but that investigation focused on other aspects of the response field, and it is of interest to ascertain whether the results of the winter season experiments are similar to those of the spring season.

In this note, we describe the sensitivity of Amazon Basin rainfall to heating imposed over the western tropical Pacific (section 2), and to cooling imposed in the eastern Pacific Ocean (section 3). The time evolution of the latter experiments is studied in section 4 in order to infer whether the South American response is a simple direct consequence of the Walker cell that propagates eastward from the Pacific heating modifications, or whether this is a more complex response involving midlatitude teleconnections and the circu-

Corresponding author address: Dr. Jan Paegle, Dept. of Meteorology, The University of Utah, 819 William Browning Building, Salt Lake City, Utah 84112.

lation of the North Atlantic as envisioned by Namias (1972) and Moura and Shukla (1981).

The latter studies emphasized long-term averages. However, as noted by Namias (1972), the North Atlantic–North Brazil teleconnections have "been found to characterize monthly and seasonal patterns as well as 5-day patterns." Consequently, it may be reasonable to search for these structures in real-data integrations of 10–20 days duration.

Buchmann et al. (1986) studied the strength of the Pacific–Amazon teleconnection in the National Center for Atmospheric Research Community Forecast Model (NCAR CFM) using an ensemble of ten real-data cases selected from the Global Weather Experiment (GWE). One set of forecasts, constituting the "control" sample, was initialized with real data, and used the model physics in an unmodified form. Another set of forecasts was identical to the control sample, except that an extra heating term was added to the thermodynamic equation. This term maximized just south of the equator, approximately 3000 km west of Ecuador. Another set of experiments placed the same heating anomaly slightly north of the equator and west of Central America.

These forecasts, and a similar set of experiments for the North Pacific (Paegle et al. 1987, hereafter referred to as II) are consistent with the previously cited climatological studies in that they indicate suppressed precipitation for northern sections of tropical South America associated with enhanced heating and precipitation over the eastern Pacific.

The experiments displayed the suppression of Amazon Basin rain within 5 days of Pacific heating onset. This rapid response was interpreted in terms of the eastward spread of subsidence in a region of equatorially trapped upper tropospheric westerlies that develop east of the heating modification. The subsiding, forward edge of the westerlies propagates eastward at a rate of 30–40 m s^{-1}, and possesses a structure suggestive of an equatorially trapped Kelvin wave. The resulting eastern portion of the Walker cell response encircles more than half the globe after 10 days.

An alternative explanation for the Amazon rainfall suppression is given by Namias (1972). He suggests that episodes of reduced North Atlantic cyclones occur with suppressed rainfall in northeast Brazil. In II, it is shown that the eastern North American and Atlantic troughs forecast by the NCAR CFM weaken during periods of enhanced tropical heating of the east Pacific, and the rainfall over equatorial sections of South America also weakens in these circumstances. Those forecasts support potential roles for both the Walker cell and the Namias teleconnection mechanisms. Since the former mechanism is a consequence of eastward development of Kelvin waves (Geisler 1981), while the latter is a consequence of a meridional Hadley cell teleconnection, the two explanations are quite distinct. It is useful to inquire which is most important to present model results.

2. Far west heating experiments

The experiments use the NCAR CFM, which is described in more detail in section 2 of I. This spectral model employs a rhomboidal truncation at wavenumber 15, and incorporates fairly complete physics parameterizations. It is initialized from ten different initial winter dates starting in December 1978 and continuing into February 1979. The same dates were selected to initialize the experiments described in I and II. The interval includes the first special observing period (SOP-1) of the GWE, and provides an unusually high quality dataset. The cases were originally selected on the basis of their rather distinct synoptic weather regimes (see Baumhefner 1984). The availability of a number of distinct cases is important for present goals because of the sensitivity of tropical prediction to weather regime.

Figure 1a shows the 10-day averaged precipitation for the case initialized on 8 January 1979. This figure displays expected distributions of tropical rainfall, with maxima over the Amazon Basin, tropical Africa and the western Pacific Ocean.

The heating field that was added to one of the experiments described in I maximizes at 105°W, just north of the equator in a region of relatively warm sea surface temperature (SST) (see Fig. 2 of I). The heating was added directly into the thermodynamic equation rather than imposed through sea surface temperature. The vertical profile of the heating function is crudely similar to the parabolic profile employed by Kasahara and Silva Dias (1986). The presently selected heating maximizes at 400 mb and is zero at 100 mb and 1000 mb. This structure imposes a somewhat deeper layer of heating than that used by Kasahara and Silva Dias (1986). Consequently, the dominant internal vertical modes excited in the present study are somewhat deeper than in their case, and the remote response may be somewhat greater.

Figure 1b displays the resulting 10-day averaged precipitation for the same initial condition as the control experiment shown in Fig. 1a, but with heating maximizing at 105°W. This shows a clear reduction of precipitation over tropical South America, and, in this sense, is typical of each of the ten cases presented in I. The remote response to a localized heat source depends upon the initial state and the location of the source because the "refractive index" for Rossby wave propagation is highly variable in time and space, (e.g., Paegle et al. 1983). The sensitivity of the response to time variations is somewhat reduced by our averages over ten distinct flow types. However, the only way to check the sensitivity to location is to move the source.

We next displaced the Pacific heating anomaly center far to the west at 6.6°S, 120°E. The resulting 10 day

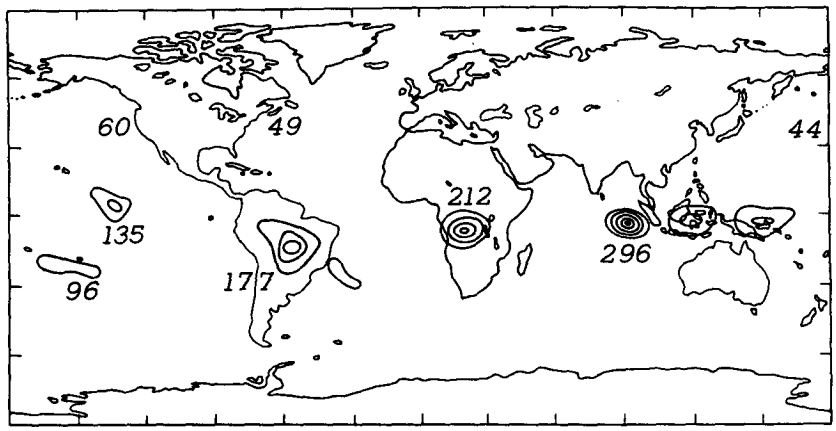

(a)

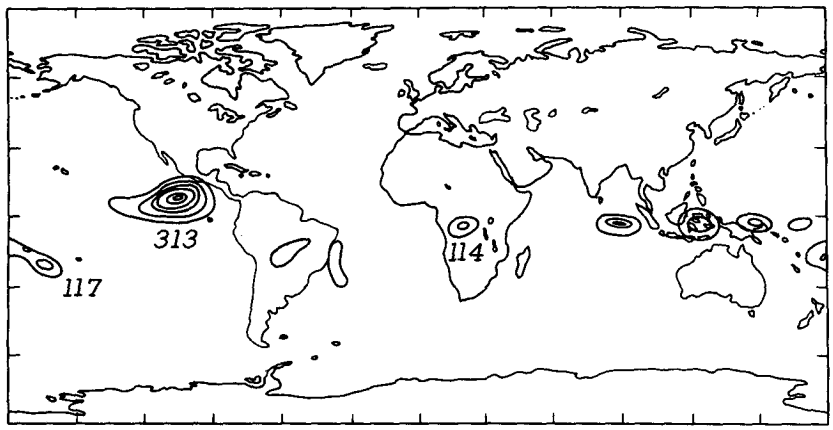

(b)

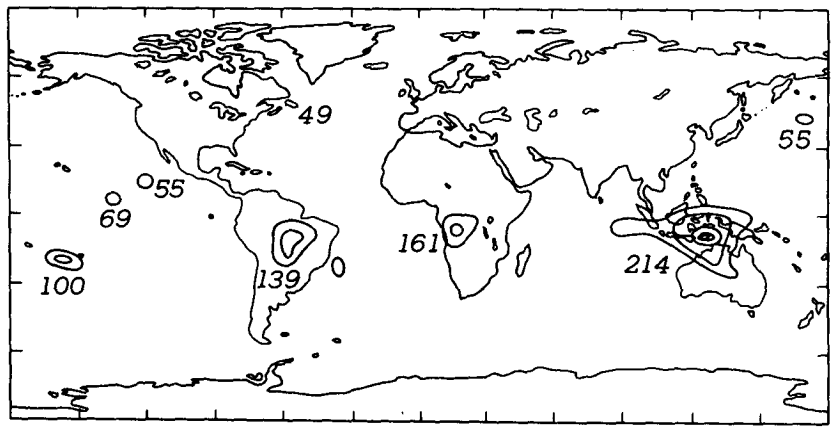

(c)

FIG. 1. Ten-day average precipitation for case initialized on 8 January 1979: (a) control; (b) experiment with east Pacific heating; (c) experiment with west Pacific heating. The maximum values are plotted and the unit is 0.01 cm day^{-1}; the contour interval is 0.5 cm day^{-1}.

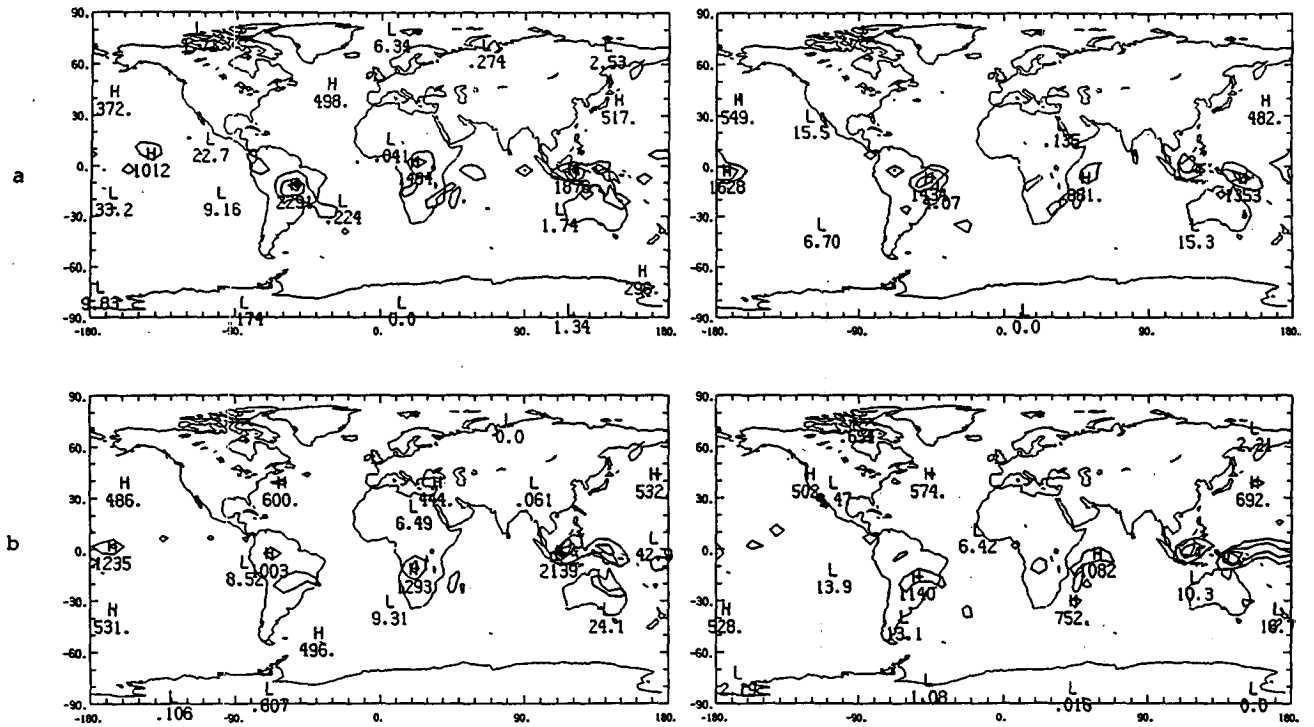

FIG. 2. Ensemble averaged precipitation for controls at (a) day 5, (b) day 10, (c) day 15, (d) day 20. The maximum values are plotted and the unit is 0.001 cm day^{-1}; the contour interval is 0.5 cm day^{-1}.

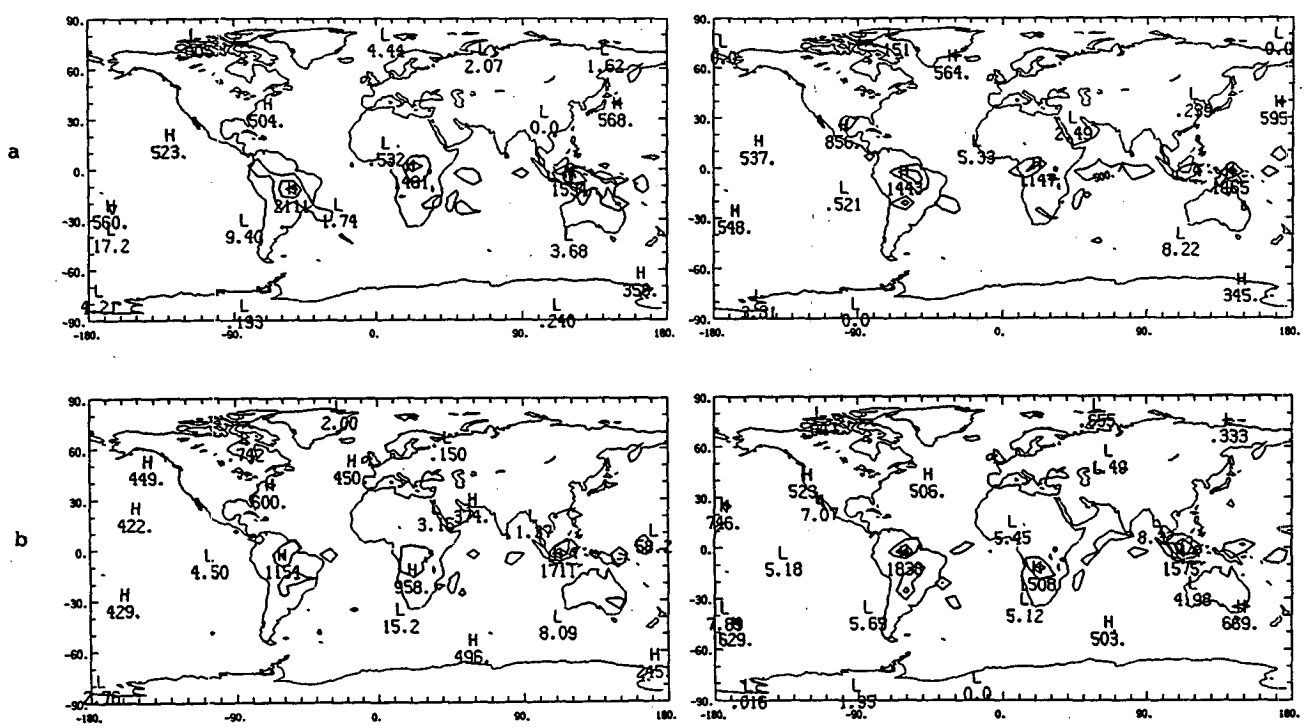

FIG. 3. As in Fig. 2, but for the experiment with reduced SST in eastern tropical Pacific.

averaged precipitation for the case initialized on 8 January 1979 is displayed in Fig. 1c. Comparing these results with Fig. 1a, it is evident that this case has reduced rainfall over the Amazon Basin with respect to the control, although this reduction is not as great as in Fig. 1b for the far eastern Pacific heating. This conclusion also holds for each of other nine cases of the ensemble. The results generalize the conclusions of I in that heating enhancements anywhere above the tropical Pacific Ocean tend to reduce the rainfall over northern Brazil in the absence of other influences.

These conclusions are superficially inconsistent with observations of wetter than normal weather over northern sections of South America during anti-El Niño phases of the Southern Oscillation–El Niño (ENSO) oscillation, (e.g., Rogers 1987) because the heating maximum shifts towards the western Pacific in such cases. However, those cases are also characterized by cooler than normal SST over the eastern Pacific, a circumstance that promotes Amazon Basin rainfall in the northern spring CFM integrations presented in II. It is important to test the generality of these conclusions for other seasons.

3. Effect of reduced sea surface temperature

The purpose of the present section is to describe the influence of reduced eastern Pacific SST during the northern winter. The SST modification is centered near the equator at 135°W. Following II, we use a rather exaggerated anomaly that peaks at −10°C in order to completely suppress tropical rainfall over the region of maximum temperature drop. This decreases to a 5°C SST reduction 3000 km from the maximum change with a Gaussian dependence on radial distance. We have not performed sensitivity tests for weaker modifications.

Figures 2 and 3 display the composite average of the precipitation at days 5, 10, 15 and 20 of the controls and experiment, respectively. The tropical rainfall over the eastern Pacific has clearly diminished as a consequence of the reduced SST. The effect over South America is not equally obvious, but close scrutiny of the diagrams suggests a northward shift in the experiments with respect to the controls. This shift is present at day 5, but is more obvious on days 10, 15 and 20.

The result may be compared with observations of Rogers (1987) and Aceituno (1988) which suggest increased (decreased) precipitation northward of approximately 8°S in association with high (low) indices of the Southern Oscillation. Since the high indices are more common during anti-El Niño years that have relatively cold east Pacific SST, it appears that the present results are consistent with observations. Rogers' (1987) and Aceituno's (1988) results are statistically significant only over restricted portions of tropical South America. Present results are also consistent with this. Figures 4a–c display regionally enhanced precipitation distribution of the control, the experiment and

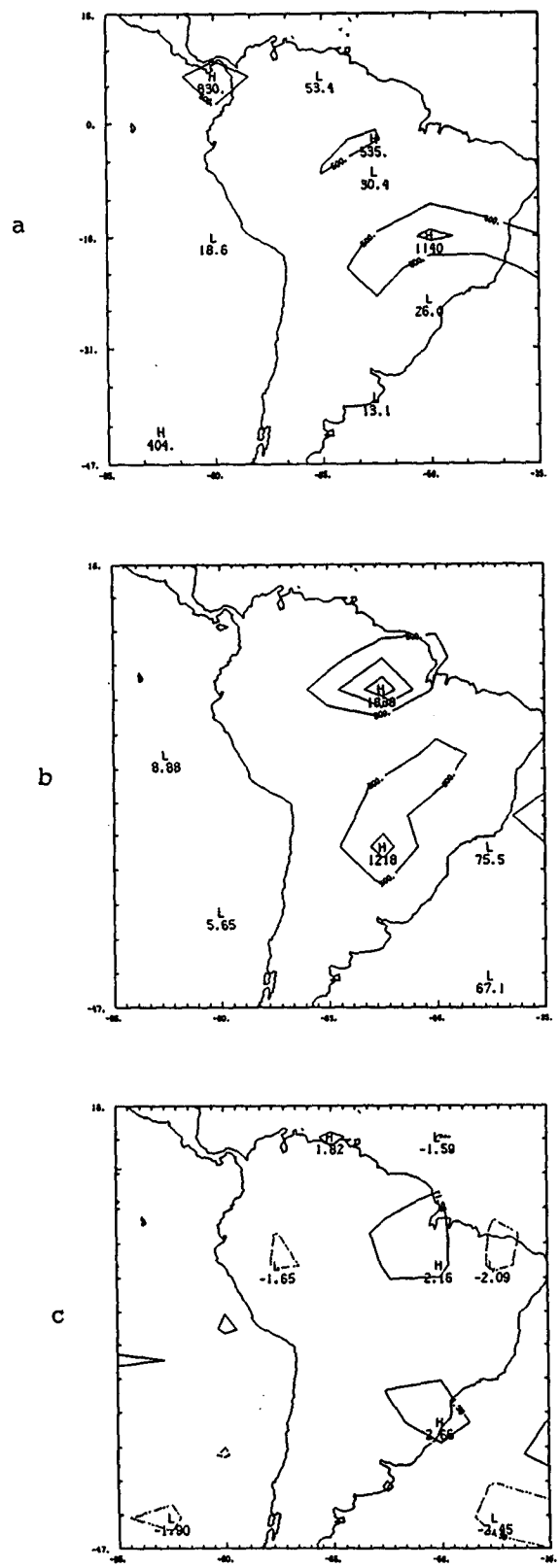

FIG. 4. Regional enhancement of (a) Fig. 2d and (b) Fig. 3d. (c) The t-statistic for the difference of the reduced SST experiment minus the control for day 20.

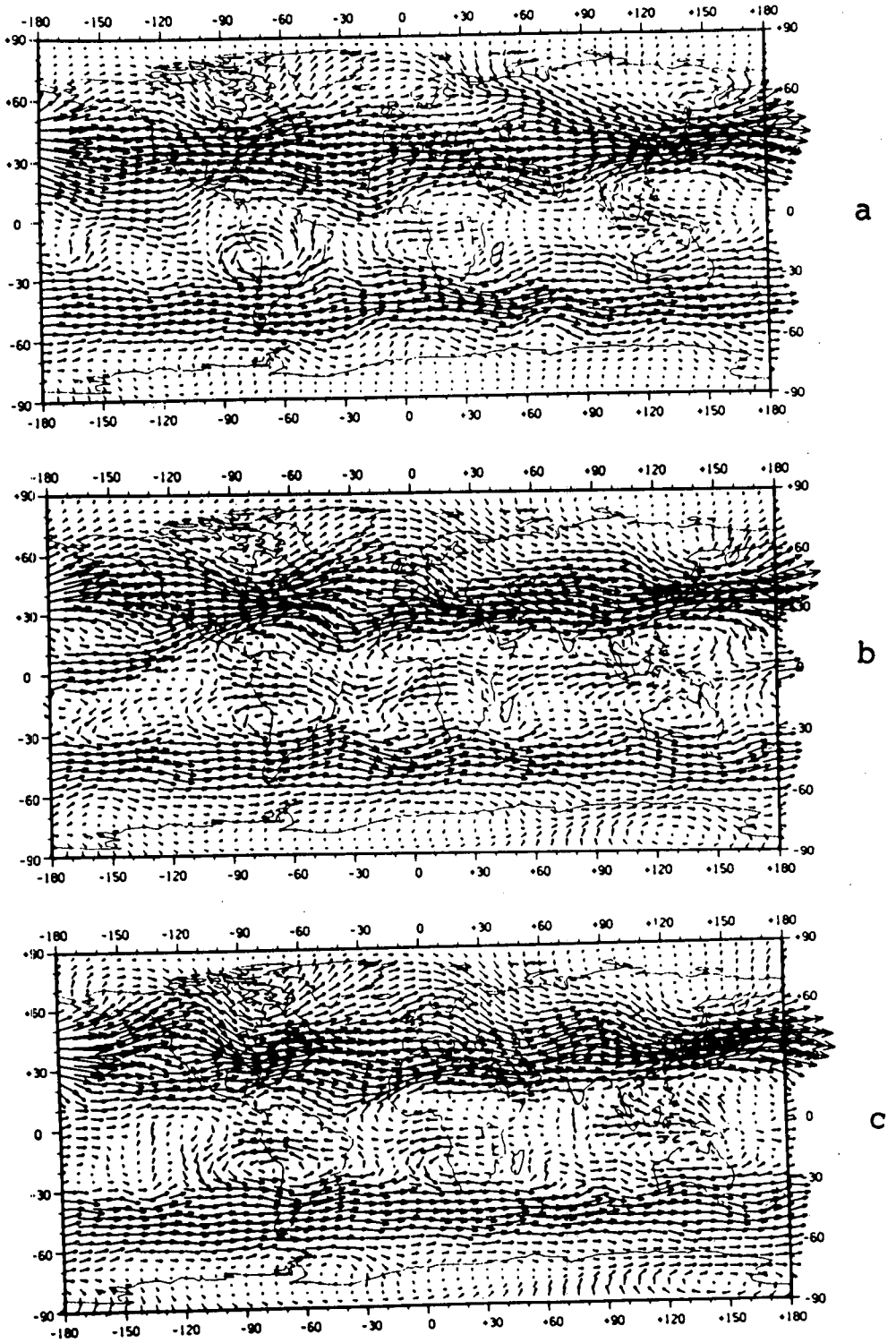

FIG. 5. The ensemble averaged 200 mb wind vector at (a) 5 days; (b) 20 days for the experiment with reduced Pacific SST; (c) 20 days for the control. The peak vector is 60 m s^{-1}.

the *t*-test of the difference (see II for *t* statistic definition) on day 20. The peak response of 2.1 in the *t* statistic over northern South America is significant at the 95% confidence level. The region of rainfall decrease located east of this position corresponds to an area where the actual rainfall is quite small in both experiment and

control, and its large t value is an artifact of small variance in this region. We conclude that there is only a 5% likelihood that the much wetter region of northern South America is purely a consequence of sampling fluctuation rather than a physical response of the forecast model.

The rainfall also appears to increase over portions of southern Brazil, extending to northern Argentina (compare Figs. 3a and 3b). This increase is not consistent with observations that show a reduction of precipitation over this area in anti-El Niño years (Aceituno 1988). However, this response is not as pronounced as the consistent response located over northern South America.

4. Evolution of circulation

In order to evaluate the relative roles of the Walker and Hadley circulation, it is useful to study the circulation changes for the integrations of the last section.

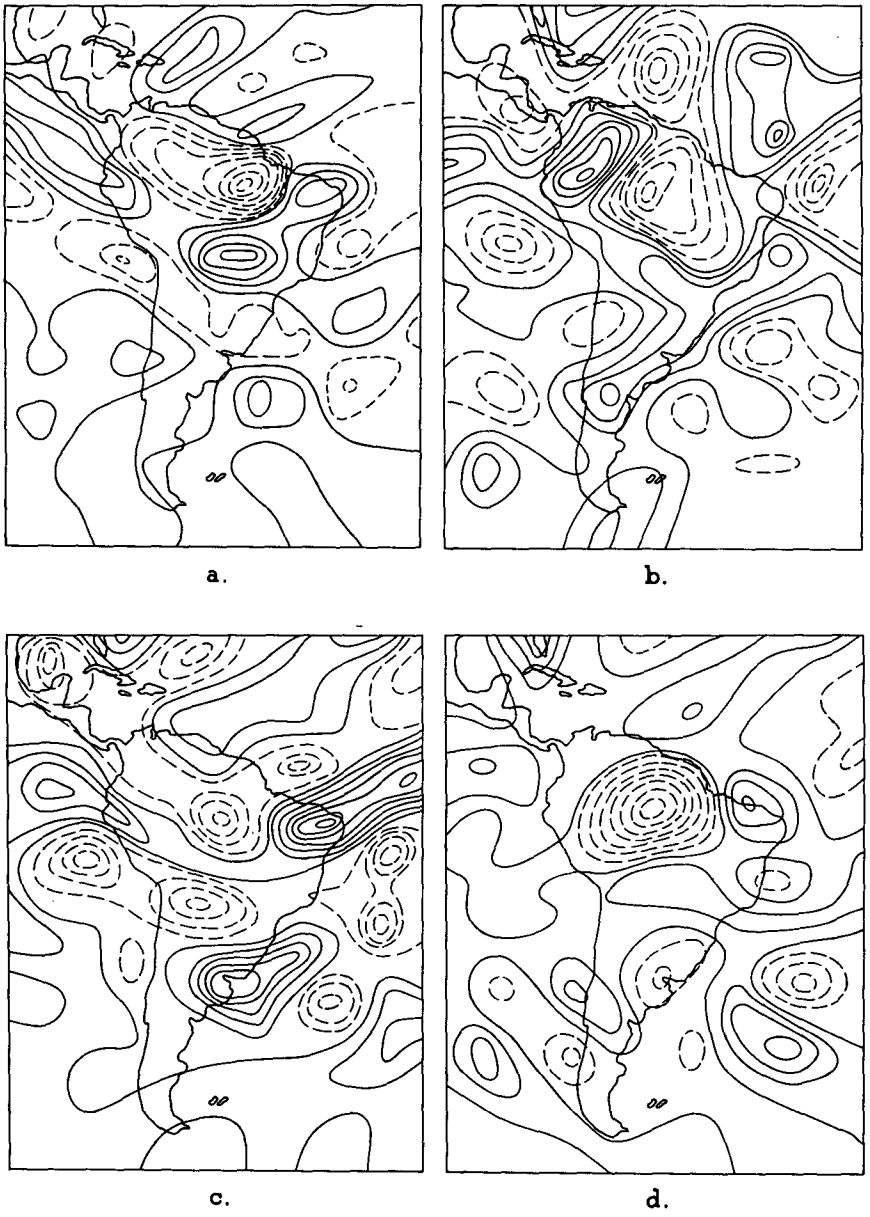

FIG. 6. Vertical motion field difference (reduced SST experiment − control) at (a) 5 days, contour interval is 1×10^{-4} mb s^{-1}, (b) 10 days, contour interval 2×10^{-4} mb s^{-1}, (c) 15 days, contour interval 3×10^{-4} mb s^{-1}, (d) 20 days, contour interval 4×10^{-4} mb s^{-1}.

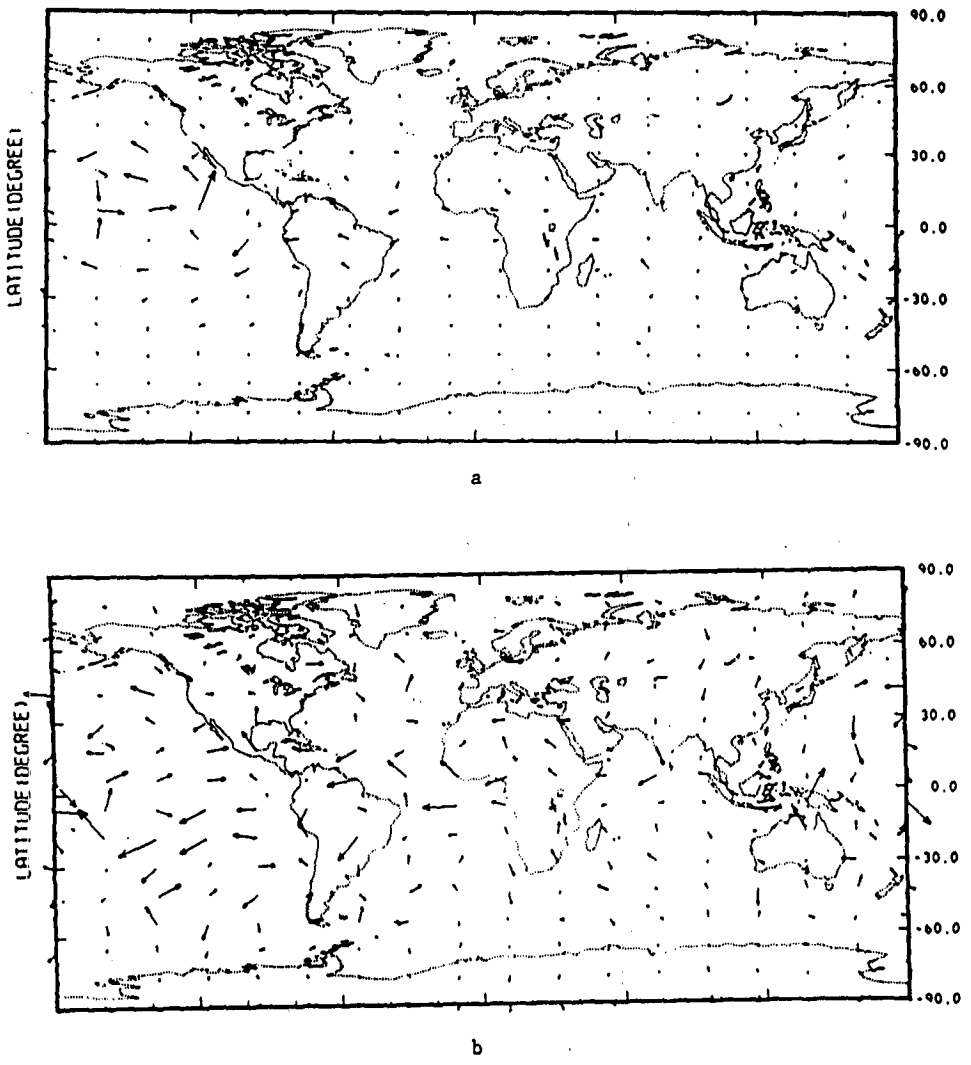

FIG. 7. Ensemble averaged 200 mb vector wind difference (reduced SST experiment − control) at (a) 5 days, peak vector 6.2 m s^{-1}, (b) 10 days, peak vector 10.1 m s^{-1}, (c) 15 days, peak vector 15.3 m s^{-1}, (d) 20 days, peak vector 20.7 m s^{-1}.

Figures 5a and 5b display the 200 mb flow field for the experiment at days 5 and 20. The pattern contains three equatorial easterly wind maxima just to the west of the region with maximum precipitation, at day 5, and this gradually deforms with time to a broad band of easterly winds emanating from the western Pacific across the Indian Ocean, Africa and South America. This produces a large inverted Walker circulation with respect to the cases forced with East Pacific heating.

The present model has a climate drift in the vicinity of the Amazon Basin that tends to displace the upper tropospheric anticyclone centered over Bolivia (the Bolivian high) west of its climatological position. This drift also tends to accentuate equatorial easterlies in the upper troposphere. Some of these features are apparent in Fig. 5c, which presents the 200 mb wind field averaged over the control ensemble for day 20. Comparing Fig. 5b with Fig. 5c suggests that most of the tropical easterly acceleration of Fig. 5b is a consequence of the heating changes, and not merely the model climate drift.

Such a large-scale effect could produce rainfall modifications over broad areas. It is interesting to note that the rainfall over Africa also increased in the experiment (compare Figs. 2 and 3). Figure 6 displays the difference in the ensemble averaged vertical motion field at 500 mb between the control and the experiment at days 5, 10, 15 and 20. The experiment shows a distinct tendency for enhanced rising motion over northern Brazil, starting at day 5 and continuing through the period. This region is in approximate correspondence with the northward shift of the precipitation indicated

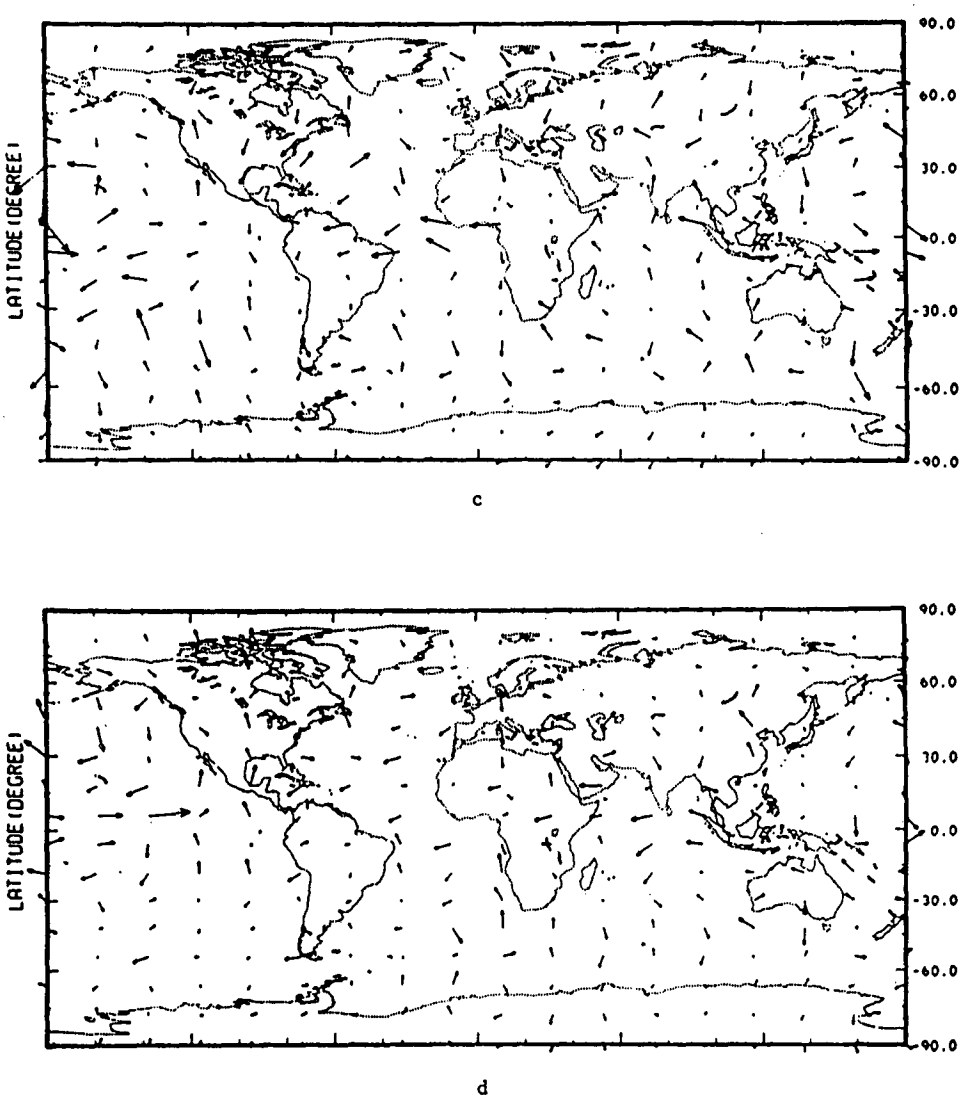

FIG. 7. (*Continued*)

in Figs. 2 and 3. Other regions also display large changes of the vertical motion field. These are probably due to changes of the global wave patterns.

It is interesting to compare the evolution of the 200 mb horizontal flow response (Fig. 7) with the vertical motion response in Fig. 6. The horizontal flow changes in Fig. 7 show almost no signal over the North Atlantic at day 5, although there is a vertical motion response over tropical South America at this time in Fig. 6. It therefore appears that the initial enhancement of rainfall over northern Amazonia is more closely linked to east–west circulation with the Pacific sector rather than to north–south connections with the Atlantic sector. Although the Hadley circulation modifications mentioned in the introduction may play a role at later times (when the North Atlantic response is large), it appears to play only a slight role in the early stages of the forecasts. However, even at later times it is difficult to identify the North Atlantic anomaly indicated by Namias (1972). Of course, these results do not refute Namias' hypothesis, which emphasizes the North Atlantic as the origin of the anomaly pattern. They do suggest that the North Atlantic anomaly is not directly connected with anomalies in the tropical Pacific, and imply that the tropical Pacific and extratropical Atlantic teleconnections have distinct origins.

5. Conclusions

The present integrations, as well as those presented in I and II, show that the NCAR CFM tends to suppress rainfall over Brazil as a consequence of heating increase occurring either nearby or more remotely over the Pacific Ocean. The suppression is relatively weaker for

more distant heating. Cooling the east-central Pacific sector produces rainfall increases over the northern sections of South America.

The evolution of these patterns agrees with the study by Walker (1928), suggesting that droughts in the northeast of Brazil are more common at certain phases of the Southern Oscillation. Others have identified these phases with El Niño episodes and increased North Pacific heating. Our results are also consistent with recent work of Rogers (1987) and Aceituno (1988). As pointed out in section 3, statistical reliability of these model results is similar to that of the observational studies.

The results may also have implications for medium term prediction of tropical rainfall, particularly in association with the 30–60 day oscillation. This oscillation usually commences as a strong convective pulse over the Indian Ocean and spreads eastward toward the eastern Pacific Ocean. The calculations of section 2 suggest that strong 30–60 day oscillations should be accompanied by suppression of the rainfall in northern Amazonia up to the time that the convective pulse passes the eastern Pacific. Furthermore, when the eastern Pacific SST is sufficiently cold to suppress this convective advance, Amazon Basin rainfall may increase relatively soon (i.e., within 5 days) with respect to the initiation phase of the 30–60 day oscillation. This inference remains to be tested in observational studies. It would also be useful to ascertain whether a significant fraction of Amazon Basin rainfall variance can be explained by the latter oscillation or by other mechanisms more internal to the basin.

Acknowledgments. This research was performed while the first author was visiting the National Center for Atmospheric Research, which is supported by NSF. The availability of computing facilities and the NCAR CFM are gratefully acknowledged. We benefited in discussions with H. van Loon, V. E. Kousky, John Horel; Pat Kennedy and R. Wolski provided much assistance. Several helpful comments were given by P. L. Silva Dias and an anonymous reviewer. This research was partly supported by NSF Grants INT 8602690 and ATM 8611952 to the University of Utah and Grant CNPq. Process n 40.2595/86 in Brazil.

REFERENCES

Aceituno, P., 1988: On the functioning of the Southern Oscillation in the South American sector. *Mon. Wea. Rev.*, **116,** 505–524.

Aragoa, J. O. R., 1986: A general circulation model investigation of the atmospheric response to El Niño. Cooperative Thesis No. 100, NCAR/CT-100 [Available from librarian, NCAR, Boulder, Colorado, 80307, U.S.A.]

Baumhefner, D. P., 1984: Analysis and forecast intercomparisons using the FGGE SOP-I data base. FGGE Workshop Rep., Woods Hole, MA, National Academy of Sciences, 228–246. [Available from USC-GARP (JH 810) National Academy of Sciences, 2101 Constitution Ave., Washington, D.C., 20418.]

Buchmann, J., L. E. Buja, J. Paegle, C. D. Zhang and D. P. Baumhefner, 1986: FGGE forecast experiments for Amazon Basin rainfall. *Mon. Wea. Rev.*, **114,** 1625–1641.

Geisler, J. E., 1981: A linear model of the Walker Circulation. *J. Atmos. Sci.*, **38,** 1390–1400.

Hastenrath, S., and L. Heller, 1977: Dynamics of climatic hazards in Northeast Brazil. *Quart. J. Roy. Meteor. Soc.*, **35,** 77–92.

Kasahara, A., and P. L. Silva Dias, 1986: Response of planetary scale waves to stationary heating in a global atmosphere with meridional and vertical shear. *J. Atmos. Sci.*, **18,** 1893–1911.

Kousky, V. E., M. T. Kagano and I. F. A. Cavalcanti, 1984: A review of the Southern Oscillation: Oceanic-atmospheric circulation changes and related rainfall nomalies. *Tellus,* **36A,** 490–504.

Moura, A. D., and J. Shukla, 1981: On the dynamics of droughts in northeast Brazil: Observation, theory and numerical experiments with a general circulation model. *J. Atmos. Sci.*, **38,** 2653–2675.

Namias, J., 1972: Influence of Northern Hemisphere general circulation on drought in Northeast Brazil. *Tellus,* **24,** 336–343.

Paegle, J., J. N. Paegle and Y. Hong, 1983: The role of barotropic oscillations within atmospheres of highly variable refractive index. *J. Atmos. Sci.*, **40,** 2251–2265.

——, C. D. Zhang and D. P. Baumhefner, 1987: Atmospheric response to tropical thermal forcing in real data integrations. *Mon. Wea. Rev.*, **115,** 2975–2995.

Rogers, J. C., 1987: Variability in clouds and precipitation over South America and the tropical Atlantic associated with the Southern Oscillation. *Trop. Ocean–Atmos. Newslett.*, **37,** 7–10.

Ropelewski, C. F., and M. S. Halpert, 1987: Global and regional scale precipitation patterns associated with the El Niño/Southern Oscillation. *Mon. Wea. Rev.*, **115,** 1606–1625.

Walker, G. T., 1928: Ceara (Brazil) famines and the general circulation movements. *Beitr. Phys. Frein Atmos.*, **14,** 88–93.